ELSEVIER

Journal of Alloys and Compounds 321 (2001) 1–9

Journal of ALLOYS AND COMPOUNDS

www.elsevier.com/locate/jallcom

Hyperfine interaction of ^{111}Cd in Fe–Sn compounds

B. Wodniecka, P. Wodniecki*, A. Kulińska, A.Z. Hrynkiewicz

The Henryk Niewodniczański Institute of Nuclear Physics, Radzikowskiego 152, 31-342 Kraków, Poland

Received 4 August 2000; accepted 16 January 2001

Abstract

Iron–tin compounds of different stoichiometries were studied by the perturbed angular correlation method. The hyperfine interaction parameters and their temperature dependence for ^{111}Cd probes substituting for tin in $FeSn_2$, FeSn and Fe_3Sn_2 crystal lattices were determined.

Keywords: Transition metal compounds; Magnetically ordered materials; Hyperfine interactions

1. Introduction

Perturbed angular correlation (PAC) experiments on intermetallic compounds contribute to the understanding of hyperfine field behaviour in different metallic systems. The PAC technique is very sensitive to the microstructure around a probe atom and can be used to follow the changes on a microscopic scale. Each position of the probe atom relative to the neighbouring atoms usually gives its own characteristic and distinguishable signal. The electric field gradient (EFG) at a nuclear probe depends on the nearest charge distribution and its determination is an excellent tool to study the electron density which depends on the chemical composition of the material. The temperature dependence of the EFG provides a way to study the dynamics of the material structure and models have been developed to understand the behaviour of EFG with temperature. The hyperfine magnetic fields observed in ferromagnetic materials reflecting the local spin polarization of electrons associated with impurity atoms aid in the study of the details of magnetic coupling.

In our previous papers [1,2] intermetallic compounds of the Co–Sn system were studied with ^{111}Cd and ^{119}Sn probes. Fe–Sn compounds are the subject of the present paper. In the course of systematic studies on the Fe–Sn system, PAC measurements in samples with different tin concentrations were performed over a wide temperature range. The hyperfine interaction was measured using a ^{111}In(EC)^{111}Cd probe representing a dilute impurity in the system studied and therefore one can observe that some of the crystallographic sites are preferred by the probes. The measured hyperfine interaction parameters were compared with the PAC findings for Co–Sn isostructural compounds [1,2] and with the results of ^{119}Sn Mössbauer spectroscopy [3,4].

2. Experimental

Iron–tin samples of different stoichiometries ($FeSn_2$, FeSn, Fe_3Sn_2 and Fe_5Sn_3) were obtained by melting, under argon atmosphere, appropriate amounts of high-purity iron and tin with ^{111}In activity, followed by annealing in evacuated and sealed quartz tubes.

PAC spectra were measured with a standard slow–fast coincidence setup with four BaF_2 detectors positioned at relative angles of 180 and 90°. The measurements were performed in the temperature range 30–1100 K. For PAC measurements below room temperature a closed-cycle helium refrigerator was used. The experiments above 300 K were carried out using a small resistive vacuum oven.

Analysis of all experimental $R(t)$ spectra, taken above the Néel temperatures of the compounds studied, was performed assuming the expression of the perturbation factor $G_2(t)$ [5] valid for static electric hyperfine interactions in polycrystalline samples:

$$G_2(t) = \sum_{i=1}^{k} f_i \sum_{n=0}^{3} s_{2n}(\eta_i) \cos(g_n(\eta_i)\nu_{Qi}t) \exp(-g_n(\eta_i)\delta_i t) \quad (1)$$

The least squares fits of the perturbation factor to the

*Corresponding author.

E-mail address: pawel.wodniecki@ifj.edu.pl (P. Wodniecki).

0925-8388/01/$ – see front matter
PII: S0925-8388(01)00937-9

Table 1
The QI parameters for ^{111}Cd and ^{119}Sn in Fe–Sn and Co–Sn compounds

Compound	Structure type	Lattice site	$\|V_{zz}\|$ (10^{18} V cm^{-2})		η	b (10^{-5} K$^{-3/2}$) ^{111}Cd
			^{111}Cd	^{119}Sn		
FeSn	B35	2(*d*) $\bar{6}m2$	1.29(2)[a]	3.9(3)[e] [3]	0.00	0.25(1)[b]
		1(*a*) *6/mmm*	1.88(4)[a]	7.2(5)[e] [3]	0.00	0.44(1)[b]
CoSn [1,2]	B35	2(*d*) $\bar{6}m2$	1.27(3)	3.8(3)	0.00	0.26(2)
		1(*a*) *6/mmm*	1.90(4)	7.3(6)	0.00	0.36(1)
$FeSn_2$	C16	8(*h*) *m.2m*	0.70(1)	2.1(2) [4]	0.26(1)	0.29(2)[c]
$CoSn_2$ [2]	C16	8(*h*) *m.2m*	0.67(1)	1.9(2) [4]	0.39(1)	0.33(1)
Fe_3Sn_2 ht	Fe_3Sn_2 hR10	6(*c*) *3m*	1.20(1)[d]		0.00	
		6(*c*) *3m*	1.00(1)[d]		0.00	
α-Co_3Sn_2 [2]	Ni_3Sn_2	4(*c*) *.m.*	1.09(1)		0.52(2)	
		4(*c*) *.m.*	0.88(1)		0.37(2)	

[a] At 388 K.
[b] Above 380 K.
[c] Above 468 K.
[d] At 885 K.
[e] At 395 K.

experimental data yield the fractions f_i of probes exposed to different EFGs characterized by the quadrupole frequencies ν_{Qi} and asymmetry parameters η_i. Broadening of the EFG is described by the width δ_i of the Lorentzian ν_{Qi} distribution. The various observed fractions f_i with different PAC parameters indicate the population of non-equivalent probe sites in the sample.

The DEPACK program from Uppsala, calculating the general expression for combined static electric and magnetic interactions in powder samples, was used for fitting the parameters of the hyperfine interactions below the Néel temperatures. From the fitting program, the Larmor frequency ω_L, the quadrupole interaction parameters ν_Q and η, and the polar angles θ and ϕ of the magnetic field direction in the EFG tensor principal axis frame can be determined.

The EFG values shown in Table 1 were calculated from the quadrupole frequencies ν_Q

$$V_{zz} = h\nu_Q/eQ \quad (2)$$

using a quadrupole moment Q value of 0.83(13)b [6]. The hyperfine field values

$$H = hI\omega_L/2\pi\mu \quad (3)$$

were calculated from the Larmor frequencies using $\mu = -0.7656(25)\ \mu_N$.

The temperature dependence of EFG was fitted using the formula [7]

$$V_{zz}(T) = V_{zz}(0)[1 - bT^{3/2}] \quad (4)$$

3. Results and discussion

3.1. The $FeSn_2$ phase

The $FeSn_2$ phase is stable up to the peritectic temperature of 769 K [8]. The tetragonal unit cell of the C16-type structure contains four iron atoms in (*a*) sites and eight tin atoms in (*h*) sites (Fig. 1). The iron site has a high symmetry, with each Fe atom surrounded by eight Sn atoms at the corners of a square antiprism, while the tin atoms are located in a less symmetric arrangement. Iron atoms form chains parallel to the *c*-axis. Each Sn atom has four Fe nearest neighbours that belong to two neighbouring chains. The point symmetry *mm* at the Sn site allows us to deduce the directions of the principal axes of the electric field gradient tensor. One axis is parallel to [001], the second is parallel to [110] and the third to [1$\bar{1}$0] (see Fig. 2). Although it is not possible to determine a priori which is the principal *Z* axis, point charge model (PCM) calculations imply that this axis is in the (100) plane.

Viewed from the *c*-axis the magnetic structure consists of alternate antiferromagnetic iron and tin planes. $FeSn_2$ is antiferromagnetic below 378 K as deduced from a neutron diffraction experiment [9,10]. The unit cell of the antiferromagnetic array is the same as the chemical cell. Successive coordination shells of all Sn atoms are known to have a zero net moment at room temperature. A second magnetic transition occurs at $T_t = 93$ K. Between T_N and T_t the magnetic structure is collinear and characterized by ferromagnetic (100) planes, antiferromagnetically coupled along the [100] direction. It was shown [4,9] that the spin directions are in the basal plane, making an angle α with

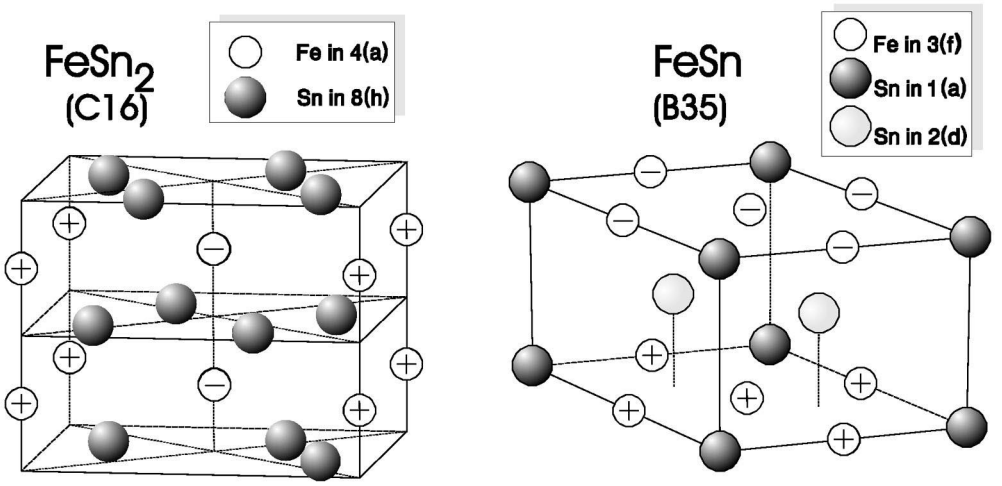

Fig. 1. Unit cells of antiferromagnetic $FeSn_2$ and FeSn compounds. The relative orientations of the Fe spins are shown.

the [100] direction, but the precise direction in the plane cannot be deduced from neutron diffraction patterns. Below T_t, $FeSn_2$ becomes non-collinear antiferromagnetic and the Fe moments would form a canted structure along the *c*-axis with canting angle 2β, making angles $\alpha + \beta$ and $\alpha - \beta$ with the [100] direction.

Between the Néel point and the second transition T_t, the collinear magnetic structure (Fig. 2) determined by neutron diffraction experiments [9] was confirmed by a Mössbauer study of $FeSn_2$ [4]. The spin direction is close to [100] at room temperature and deviates slightly when the temperature decreases to T_t. Below T_t a non-collinear structure is necessary to explain the ^{119}Sn spectra.

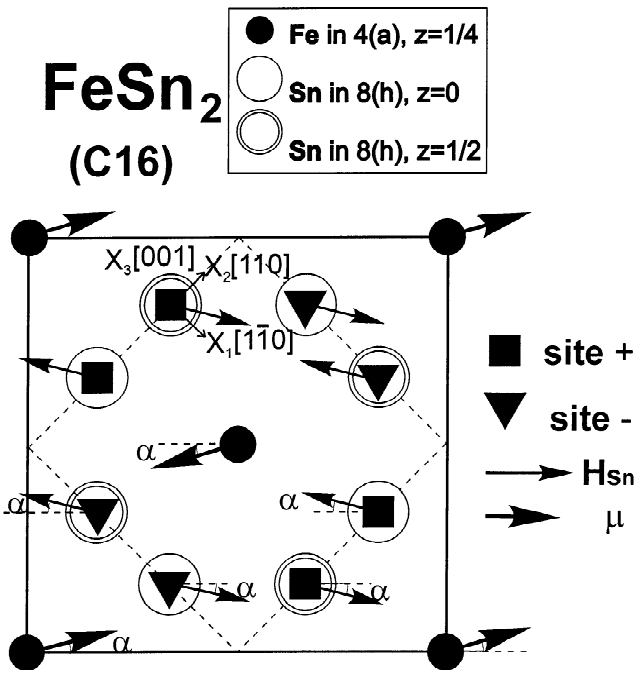

Fig. 2. The collinear antiferromagnetic structure of $FeSn_2$ above T_t [4]. The Fe magnetic moment directions and the Sn hf field directions are shown by arrows.

The $FeSn_2$ sample with 66.5 at.% Sn was melted with radioactive ^{111}In and annealed for 2 h at 700 K. Representative PAC spectra recorded for this sample are shown in Fig. 3.

At 388 K, i.e. above T_N, only one unique quadrupole interaction with a quadrupole frequency ν_Q of 142.5(3) MHz and $\eta = 0.32(1)$ was observed and related to probe atoms in the 8(*h*) position of the $FeSn_2$ phase. Fig. 4 shows the temperature changes of the fitted quadrupole interaction parameters of ^{111}Cd in the $FeSn_2$ phase. The asymmetry parameter value increases with temperature from $\eta \approx 0.15(1)$ to 0.39(1) at 760 K. The room temperature value of η calculated in the point charge model (PCM) approximation, with the assumption of charges of $Q_{Fe} \approx 2$ and $Q_{Sn} \approx 3.7$ on the Fe and Sn ions, is in agreement with the measured value of 0.26(1).

Below T_N the measured V_{zz} value increases with temperature, and above 400 K decreases following an approximate $T^{3/2}$ relation (Eq. (4)) with slope parameter $b = 0.29(2)$. In the $CoSn_2$ isostructural compound the $T^{3/2}$ character of the quadrupole frequency temperature dependence, with similar slope, was observed over the whole stability range [2]. These results differ from those for the other investigated C16 compounds, where a linear temperature dependence was found [11–13].

The determined quadrupole interaction parameters of ^{111}Cd probes in Fe–Sn and Co–Sn [1,2] compounds are compiled in Table 1, where for comparison the results for ^{119}Sn probes [1,3,4] are also presented. As can be seen from Table 1, the experimental EFG value on ^{119}Sn is three times larger than that measured on ^{111}Cd nuclei. The electric quadrupole interaction at the same probe is similar

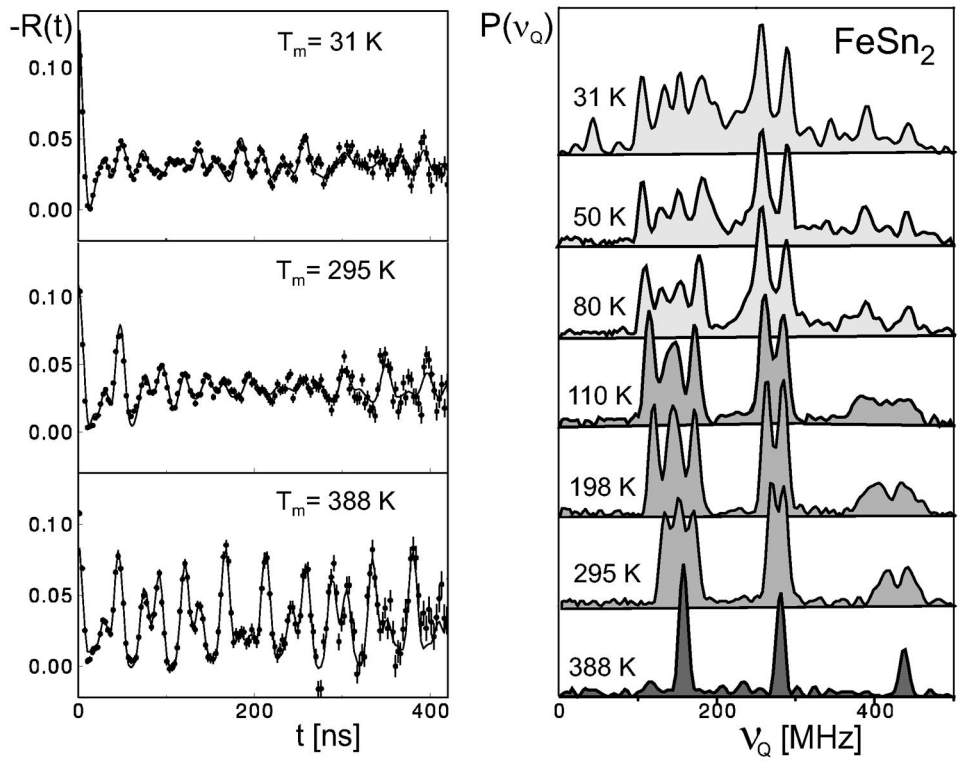

Fig. 3. PAC patterns with Fourier transforms recorded for the $Fe_{33.5}Sn_{66.5}$ sample at the T_m temperatures indicated (different shadings correspond to temperature regions: $T_m > T_N$, $T_t < T_m < T_N$, $T_m < T_t$).

in isostructural $FeSn_2$ and $CoSn_2$ compounds, which might be expected in view of the similarity in the atomic environment.

For both ^{111}Cd and ^{119}Sn probes a decrease of the V_{zz} value for $CoSn_2$ in comparison with $FeSn_2$ is observed and related to the existence of stronger covalent bonding between the probe and the first transition metal neighbours M. This covalent bonding is also considered to be the source of the non-zero transferred magnetic field at the tin sites in antiferromagnetic MSn_2 compounds. As the net moment of the successive Fe shells of Sn atoms is zero whatever the shell, the transferred hyperfine field is anisotropic [4].

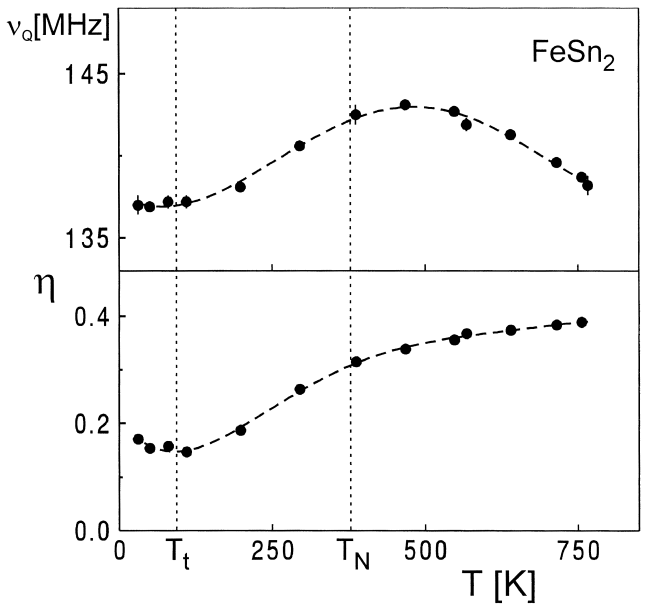

Fig. 4. Temperature dependence of the quadrupole interaction parameters for ^{111}Cd in the $FeSn_2$ phase (fits below T_N were performed assuming $\phi = 0$, see text).

Below T_N the combined interaction was evidenced in the $FeSn_2$ sample with the ^{111}Cd probe.

In the hyperfine field model, used to explain the ^{119}Sn spectra in $FeSn_2$ [4], the transferred interaction was calculated along each Sn–Fe bond considering that the anisotropic field is due to a polarization of Sn orbitals by covalency effects:

$$H = A_a \sum_{i=1}^{4} \boldsymbol{u}_i (\boldsymbol{u}_i \cdot \mu_i) \tag{5}$$

where $\boldsymbol{u}_i$ is a unit vector directed along the Sn–Fe bond and μ_i is the magnetic moment of the corresponding Fe first near neighbour of the Sn atom.

The ^{111}Cd PAC spectra recorded at temperatures between T_N and T_t could be well fitted with the assumption of the collinear magnetic structure shown in Fig. 2 with ferromagnetic (100) planes and an antiferromagnetic axis making an angle α with the [100] direction. Two probe

sites are then expected in the frame of the hyperfine field model described by Eq. (5) considering the anisotropic field resulting from covalent bonding between the transition metal and tin [4]. For "site +" (with polar angle θ^+ of the hyperfine field direction with respect to the principal 0Z axis of the EFG tensor) and for "site −" (with polar angle $\theta^- = 90° - \theta^+$) the same field $H^+ = H^-$ should be observed. The PAC patterns were well reproduced with the Larmor frequencies ω_L corresponding to the hyperfine magnetic fields H(295 K) = 6.7(2), H(198 K) = 8.9(2) and H(110 K) = 9.7(2) kG and with angles θ^+ and θ^- (where $\theta^- = 90° - \theta^+$) between $\boldsymbol{H}$ and the largest component V_{zz} of the EFG, shown in Fig. 5. The best fits were obtained assuming a polar angle ϕ of 0, i.e. the field direction in the (100) plane. These results agree with those deduced for the collinear magnetic structure of $FeSn_2$ with spin directions close to [100] deduced from a Mössbauer experiment (see Fig. 2). The deviation α of the ferromagnetic axis from [100], resulting from our measurements, is smaller than 10(5)° at room temperature and is 11(3)° and 15(3)° at 198 and 110 K, respectively. For comparison, the α values extracted from ^{119}Sn Mössbauer spectra recorded at similar temperatures are 12(2)°, 15(2)° and 18.5°(20) and the ^{119}Sn transferred hyperfine field values are ≈3.2 times higher (see Fig. 5) [4].

At 31, 50 and 80 K, i.e. below T_t, a non-collinear structure is necessary to explain the ^{111}In hyperfine interaction. These results agree with the changes observed at 93 K in magnetic, neutron diffraction and Mössbauer spectroscopy experiments [4,9]. The PAC spectra are characterized by the existence of at least two magnetic fields. Quite satisfactory fits were obtained with two magnetic fields taken into account. The fitted H^+, H^-, θ^+ and θ^- values are shown in Fig. 5 for two fit series: with equal populations $f^- = f^+$ of the two probe sites (solid circles) and for the $f^- = 2f^+$ probe fractions (empty circles). It can be seen that the H^- and θ^- values do not depend on the f^+/f^- ratio. The fitted $H^+/H^- \approx 2.0(5)$ ratio and $|\theta^-| = 28–33°$ and $|\theta^+| = 70–80°$ values, as well as the results of ^{119}Sn Mössbauer measurements [4], do not agree with the values $\alpha = 45°$ and $\beta \approx 10°$ (i.e. $H^+/H^- \approx 1.04$, $\theta^+ = 90°$ and $\theta^- = 0°$ for V_{zz} in the [110] direction or $\theta^+ = 16°$ and $\theta^- = 90°$ for V_{zz} in the [1$\bar{1}$0] direction) proposed on the basis of a neutron diffraction study [9].

Above 750 K, the decomposition of $FeSn_2$ was observed in agreement with the phase diagram.

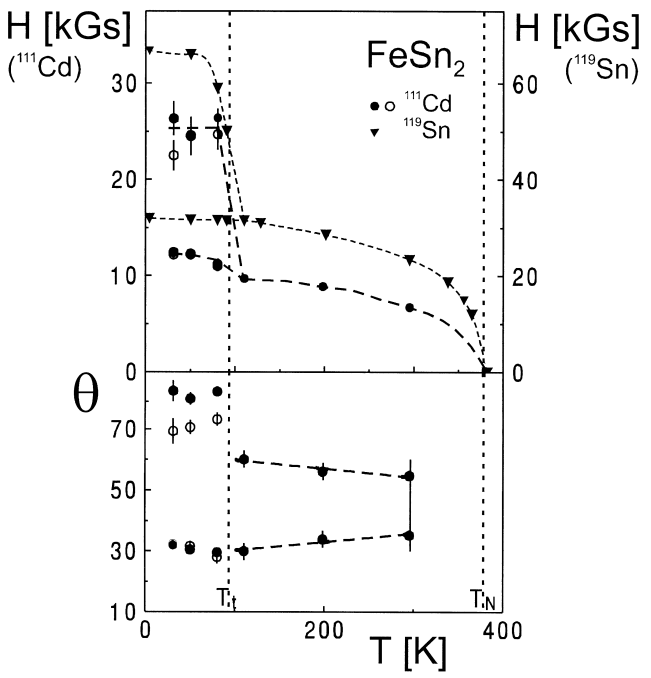

Fig. 5. Temperature dependence of the fitted ^{111}Cd hf interaction parameters in $FeSn_2$ compounds below the Néel temperature (the magnetic fields H and angles θ of the field directions in the EFG tensor principal axis frame). For comparison the ^{119}Sn hyperfine fields are also shown [4].

3.2. The FeSn phase

Hexagonal FeSn is stable up to the peritectic temperature of 1013 K [8]. In the unit cell of the B35 structure (Fig. 1) there is a three-fold position occupied by iron, while tin occupies one single-fold and one two-fold position with axial symmetry. FeSn is antiferromagnetic with a Néel temperature T_N of 368 K. Below T_N a magnetic field at the tin 1(a) position was reported [3]. The transferred hf field at this position could be caused by conduction electron polarization or the overlap of 3d wavefunctions with the s wavefunctions of the non-magnetic atom. The latter description has been used for tin as an impurity in a Co matrix. If the 5s–3d overlap mechanism is of importance in FeSn, the cause of the vanishing field of Sn in 2(d) in contrast to Sn in 1(a) would be due to iron nearest neighbours giving a canceled 5s electron spin polarization at the Sn atoms in the 2(d) position [3].

In a neutron diffraction study performed by Yamaguchi et al. [16], an antiferromagnetic ordering in the c-direction was revealed, with the iron moments in the basal plane, either in the [100] or [210] direction. The magnetic unit cell is then twice as big as the chemical unit cell, being doubled along the c-axis. Assuming that the antiferromagnetic ordering between the basal planes of FeSn is intact, the magnetic unit cell should also be extended in the a-direction in order to explain the ^{57}Fe Mössbauer spectra [3]. The investigated samples with 49.9 at.% Sn and 50 at.% Sn contained the FeSn phase with a 20% addition of $FeSn_2$. The evolution of the PAC spectra with temperature is shown in Fig. 6. Two axially symmetric and one non-axially symmetric EFG were found in the sample and related to the 2(d) and 1(a) probe sites in the B35 structure of FeSn and the 8(h) probe position in the C16 $FeSn_2$ compound, respectively (Table 1). The greater EFG of $1.88(4)\times10^{18}$ V cm^{-2} at 388 K was ascribed to the 1(a) probe position, and the lower EFG of $1.29(2)\times10^{18}$ V

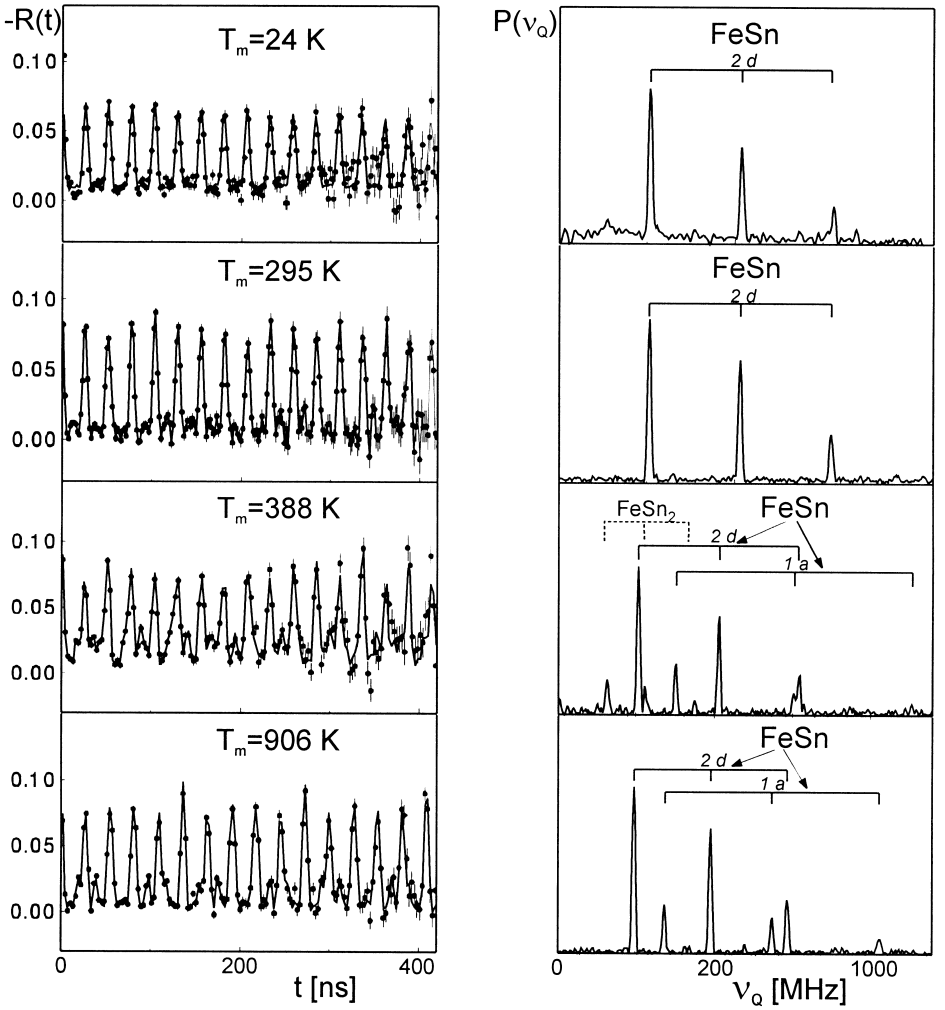

Fig. 6. PAC spectra with Fourier transforms for the $Fe_{50}Sn_{50}$ sample recorded at the temperatures indicated.

cm^{-2} to the non-magnetic 2(*d*) probe site, also taking into account the similar EFG values and their temperature dependencies observed at ^{111}Cd in isomorphic CoSn and NiIn compounds [1,2], as well as the EFG values measured at ^{119}Sn in FeSn and CoSn compounds [1,3], where the higher EFG value was found in the magnetic 1(*a*) site. In fact, below 350 K, i.e. below the Néel temperature, the hyperfine interaction of ^{111}Cd with the lower EFG, ascribed to the 2(*d*) probe site, has pure quadrupolar character (see Fig. 6). Above 760 K the decomposition of $FeSn_2$ was observed in accordance with the phase diagram. In the sample with 46.3 at.% Sn, only the two quadrupole frequencies associated with the B35 FeSn phase were observed.

A 2(*d*) site preference for Cd probes in the FeSn compound was observed (Fig. 7), contrary to CoSn, where the 1(*a*) site was populated by Cd probes more strongly than the 2(*d*) site [1].

The fitted EFG values in FeSn are very similar to those measured at ^{111}Cd in the CoSn [1] isostructural compound, which might be expected in view of the similarity both in valence electron configuration and atomic environment. These values are more than three times greater than those reported for ^{119}Sn probes in FeSn [3] (see Table 1), while

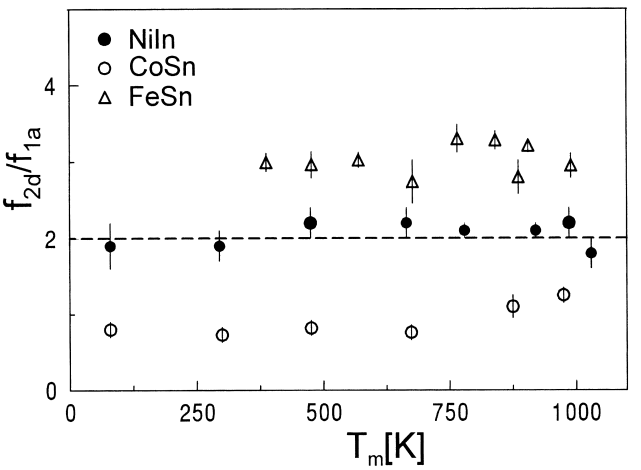

Fig. 7. The ratio of ^{111}Cd probe fractions in 2(*d*) and 1(*a*) positions of B35 phases as a function of temperature.

the ratio of the respective Sternheimer antishielding factors is 0.77. The same effect was found for isostructural CoSn [1,2] and NiIn [1] phases.

Above T_N the temperature dependence of the EFGs at ^{111}Cd in the FeSn compound, similarly as in NiIn and CoSn [2], follows a $T^{3/2}$ relation with different slope parameters b for each of the observed EFGs (see Table 1 and Fig. 8). The EFG temperature changes in B35 NiIn, CoSn and FeSn compounds are stronger for the 1(*a*) site, as well for the ^{111}Cd and the ^{119}Sn probe [1].

3.3. The Fe_3Sn_2 phase

The Fe_3Sn_2 phase has a rhombohedral structure ($R\bar{3}m$) and is reported to exist in the 880–1079 K temperature range. Fe_3Sn_2 is ferromagnetic with $T_C = 657$ K [8].

A $Fe_{60.2}Sn_{39.8}$ sample annealed for 30 h at 970 K contained the Fe_3Sn_2 phase [8] and about 30% contamination with the FeSn B35 phase.

PAC measurements performed at 885, 990 and 1016 K (Fig. 9) exhibited (besides two axially symmetric V_{zz} ascribed to the FeSn phase) two quadrupole frequencies with zero asymmetry parameters of 223(1) and 186(2) MHz at 885 K, both decreasing with temperature. This quadrupole interaction was ascribed to the 6(*c*)^{I} and 6(*c*)^{II} probe positions in the hR10 structure of the studied Fe_3Sn_2 phase.

A strong site preference for one of the two 6(*c*) positions was observed since the higher frequency was measured with a five times greater contribution. Point charge model calculations predict a greater EFG for the 6(*c*) site with more space available for the probe. Decomposition of this phase between 1016 and 1068 K was observed in accordance with the phase diagram.

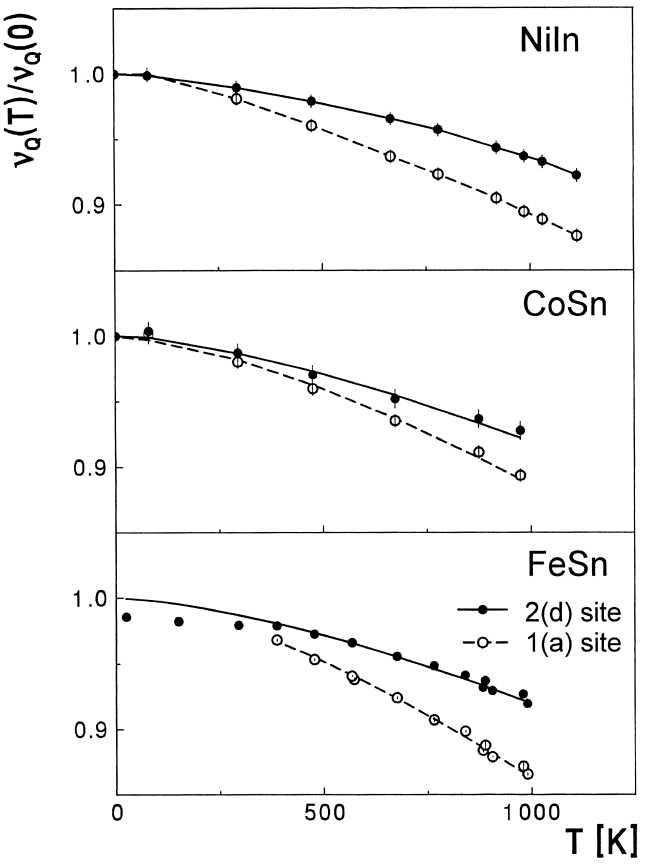

Fig. 8. Normalized temperature dependence of the quadrupole frequencies measured at ^{111}Cd in B35 compounds.

3.4. The Fe_5Sn_3 phase

The Fe_5Sn_3 high-temperature phase of the $B8_2$ structure was reported to exist within the limited temperature range of 1055 to 1183 K [8]. The PAC pattern measured for the $Fe_{62.7}Sn_{37.3}$ sample at 1077 K did not show any unique quadrupole interaction.

4. Summary

The determined quadrupole interaction parameters of ^{111}Cd and ^{119}Sn in stoichiometric Fe–Sn compounds [the experimental EFG — V_{zz}, asymmetry parameter η, and the slope parameter b of $V_{zz}(T) = V_{zz}(0)(1 - bT^{3/2})$ temperature dependence] are shown in Table 1.

In all compounds presented in Table 1, ^{111}Cd probes substitute only for Sn. However, in all compounds with more than one non-equivalent tin site, some site preference was observed. The electric field gradients measured in isostructural Fe–Sn and Co–Sn compounds are very similar, reflecting the similarity of the nearest charge distribution.

The small decrease of the V_{zz} value measured with ^{111}Cd probes in $CoSn_2$ in comparison with $FeSn_2$ can be related to the existence of covalent bonding between Cd and the first transition metal neighbours M. The covalent bonding between Sn and M, which becomes stronger in antiferromagnetic MSn_2 compounds from $MnSn_2$ through $FeSn_2$ to $CoSn_2$, is reflected both by a stronger shortening of the M–Sn shortest distance as compared with the sum of the atomic radii and by a decrease of the quadrupolar splitting of the ^{119}Sn spectra [4].

The experimental EFG values on ^{119}Sn are 2.8–3.8 times larger than those measured with ^{111}Cd probes. Comparison of the EFG magnitudes based on the semiempirical expression

$$V_{zz} = (1 - \gamma_\infty)V_{zz}^{lat}(1 - K) \quad (6)$$

requires a knowledge of the Sternheimer antishielding factors $(1 - \gamma_\infty)$. According to a tabulation of these factors for free ions [14] the ratios of the corresponding antishielding factors is 0.77. The value of $(1 - \gamma_\infty(\mathrm{Cd})) = 30$, however, is quite uncertain and, in fact, some authors [15] have indicated that a value of 16 is more appropriate.

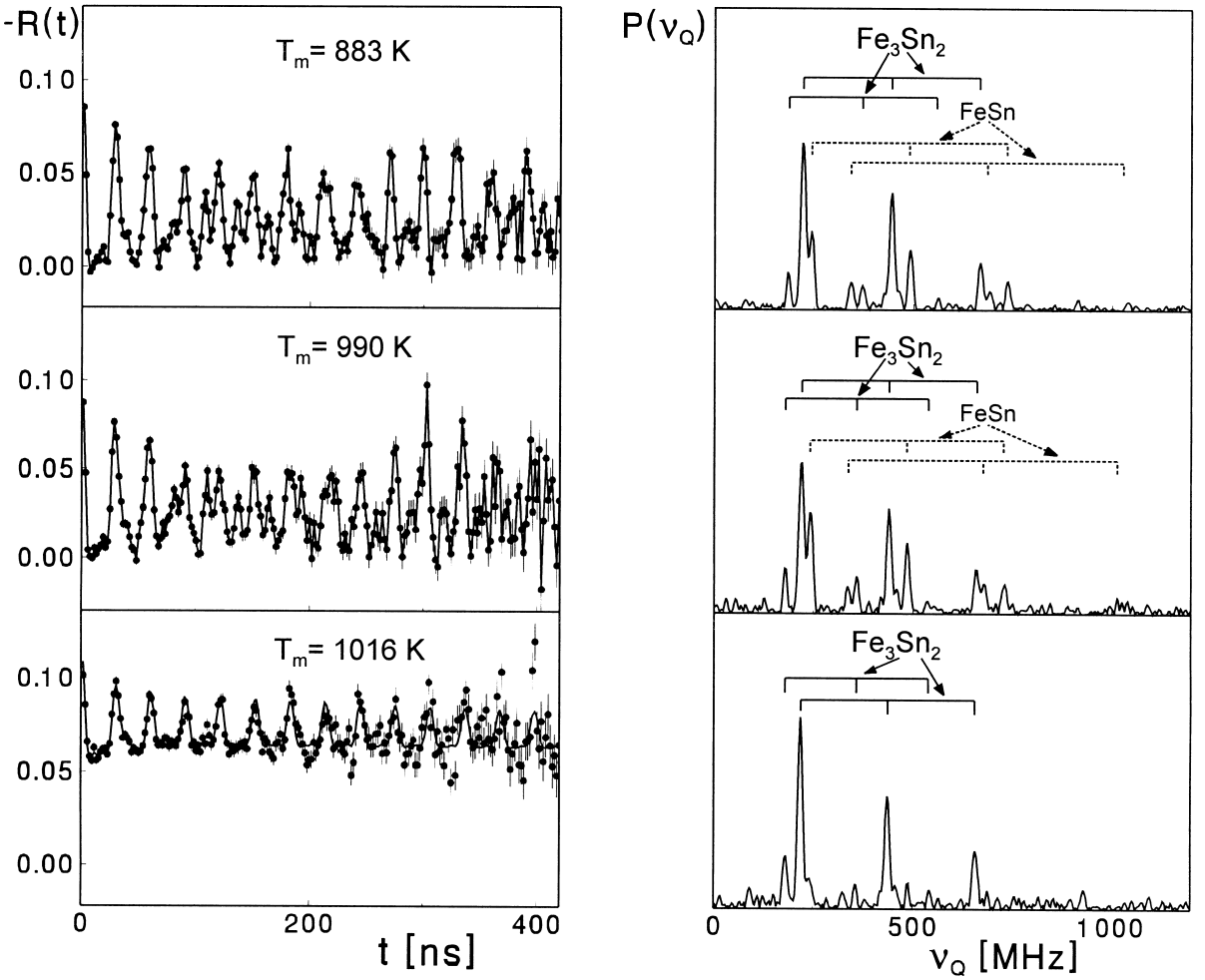

Fig. 9. PAC spectra with Fourier transform recorded for a $Fe_{60.2}Sn_{39.8}$ sample at the temperatures indicated.

Nevertheless, it does not explain the observed differences in the measured EFG values with ^{119}Sn and ^{111}Cd probes. This would lead us to the conclusion that electronics effects do not amplify the EFG by the same factor for both probes. Also, local distortions due to size mismatch and dissimilar charge screening can play a role.

Also, the hyperfine magnetic fields measured on ^{119}Sn in $FeSn_2$ are $\approx$3.2 times larger than those observed on the ^{111}Cd probe. Unfortunately, because of the strong 2(*d*) site preference it was not possible to measure B_{hf} on ^{111}Cd in the 1(*a*) site of the FeSn compound.

The results of the ^{111}Cd PAC measurements on $FeSn_2$ are in agreement with the magnetic structure deduced from a neutron diffraction study and Mössbauer experiments. They confirm the collinear magnetic structure of $FeSn_2$ between T_t and T_N with iron moment directions in the (001) plane making angles α with the [100] axis of about 10° at room temperature. A gradual rotation of the antiferromagnetic axis away from [100] is observed when the temperature decreases. Below T_t a non-collinear structure is necessary to explain the ^{111}Cd PAC spectra, which can be quite satisfactory fitted with the assumption of two magnetic fields. However, the fitted H and θ values do not agree with those resulting from $\alpha = 45(5)°$ and canting angle $\beta = 10°$ proposed on the basis of a neutron diffraction study [9]. It should be noted that the results of ^{119}Sn Mössbauer measurements are also in disagreement with $\alpha = 45°$ and $\beta = 10°$ values.

Acknowledgements

This work was supported, in part, by the Polish State Committee for Scientific Research (grant No. 2 P03B 066 18).

References

[1] B. Wodniecka, K. Tomala, P. Wodniecki, M. Marszałek, R. Kmieć, A.Z. Hrynkiewicz, Hyperfine Interactions 110 (1997) 183.
[2] P. Wodniecki, B. Wodniecka, A. Kulińska, A.Z. Hrynkiewicz, J. Alloys Comp. 264 (1998) 14.

[3] L. Häggström, T. Ericsson, R. Wäppling, E. Karlsson, K. Chandra, J. Phys. (Paris) Colloq. 35 (1974) C6–C603.
[4] G. Le Caër, B. Malaman, G. Venturini, D. Fruchart, B. Roques, J. Phys. F: Met. Phys. 15 (1985) 1813.
[5] H. Frauenfelder, R.M. Steffen, in: K. Karlsson, E. Matthias, K. Siegbahn (Eds.), Perturbed Angular Correlations, North-Holland, Amsterdam, 1963.
[6] P. Raghavan, At. Data Nucl. Data Tables 42 (1989) 189.
[7] J. Christiansen, P. Heubes, R. Keitel, W. Klinger, W. Loefler, W. Sandner, W. Witthuhn, Z. Phys. B 24 (1976) 177.
[8] H. Okamoto, T.B. Massalski, Binary Alloy Phase Diagrams, 1987.
[9] G. Venturini, D. Fruchart, J. Hübsch, G. Le Caër, B. Malaman, B. Roques, J. Phys. F: Met. Phys. 15 (1985) 427.
[10] P.K. Iyengar, B.A. Dasannacharya, P.R. Vijayaraghavan, A.P. Roy, J. Phys. Soc. Jpn. 17 (1962) 247.
[11] M. Behar, L.G. Brunnet, J.A.H. da Jornada, R.P. Livi, F.C. Zawislak, Hyperfine Interactions 15/16 (1983) 261.
[12] B. Wodniecka, M. Marszałek, P. Wodniecki, A.Z. Hrynkiewicz, Hyperfine Interactions 80 (1993) 1039.
[13] H.M. Petrilli, M. Marszałek, H. Saitoivitch, Z. Naturforsch. 51a (1996) 437.
[14] F.D. Feiock, W.R. Johnson, Phys. Rev. 187 (1969) 39.
[15] T.P. Das, M. Pomerantz, Phys. Rev. 123 (1961) 2070.
[16] K. Yamaguchi, H. Watanabe, J. Phys. Soc. Jpn. 22 (1967) 1210.